CHINESE OPTICS LETTERS

Vol. 19, No. 4 | April 2021

Wavelength-flexible all-polarization-maintaining self-sweeping fiber laser based on intracavity loss tuning

Kaile Wang (王凯乐)[1,2], Zengrun Wen (温增润)[1,2], Haowei Chen (陈浩伟)[1,2**], Baole Lu (陆宝乐)[1,2*], and Jintao Bai (白晋涛)[1,2]

[1] State Key Laboratory of Photoelectric Technology and Functional Materials, International Collaborative Center on Photoelectric Technology and Nano Functional Materials, Institute of Photonics & Photon-technology, Northwest University, Xi'an 710069, China

[2] Shaanxi Engineering Technology Research Center for Solid State Lasers and Application, Provincial Key Laboratory of Photo-electronic Technology, Northwest University, Xi'an 710069, China

*Corresponding author: lubaole1123@163.com

**Corresponding author: 67892020@qq.com

Received August 13, 2020 | Accepted October 9, 2020 | Posted Online January 8, 2021

We reported a wavelength-flexible all-polarization-maintaining self-sweeping fiber laser based on the intracavity loss tuning brought by the bent optical fiber. The bidirectional cavity structure achieved the self-sweeping effect due to the appearance of the dynamic grating in the active fiber with the spatial hole burning effect. Under this, a section of fiber was bent into a circle for adjusting the loss of the cavity. With a descending diameter of bent fiber circle, the sweeping range moves to the shorter wavelength and covers a wide range from 1055.6 to 1034.6 nm eventually. Both the initial wavelength of self-sweeping regime and the threshold of the fiber laser show exponential correlation with the diameter of the circular fiber. Our work provides a compact and low-cost way to achieve the broad wavelength-flexible self-sweeping operation.

Keywords: fiber laser; self-sweeping effect; bidirectional cavity; flexible wavelength; all-polarization maintaining.

DOI: 10.3788/COL202119.041401

1. Introduction

Among the numerous tunable fiber lasers, the self-sweeping (aka "self-induced laser line sweeping") fiber laser is quite interesting due to its exotic spectral and temporal dynamics. The self-sweeping effect was first, to the best of our knowledge, revealed in a ruby laser in 1962[1]. Kir'yanov *et al.* reawakened this field by a GTWave ytterbium-doped fiber laser with a Fabry–Perot cavity after nearly half a century[2]. Then, the self-sweeping effect was deeply studied in the fiber waveguides via the constant dedication of a few experienced teams. Hitherto, the self-sweeping fiber laser has contributed tremendous advances in fundamental physics and applications.

Over the past decade, the self-sweeping fiber laser has experienced a rapid growth that focused on the theory and experimental study. The initial research was located on the Yb-doped fiber laser[3,4]. Lobach *et al.* not only found the microsecond pulse that arises from the self-sustained relaxation oscillations but also summed up the behaviors of the self-sweeping effect on a large number of experiments and further proposed the non-stationary spatial hole burning model to describe the laser frequency dynamics[5]. Peterka *et al.* deduced the grating spectra in simulation based on the distribution of refractive index change along with the active fiber, and the further results showed a wavelength difference between the peak of reflectivity spectra and the operating wavelength[6,7]. Then, Drobyshev *et al.* reconstructed the spectrum of a gain grating in the experiment, while the spectral width of 50 MHz and reflectivity of ~0.1% were confirmed[8]. Meanwhile, the single-period sweeping range of self-sweeping Yb-doped fiber laser can be optimized to 21 nm[9]. The largest coverage ranges from 1045 nm to 1087 nm via the Lyot filter[10]. Ultra-stable spectral periods also can be obtained by use of the Michelson configuration[11]. The above achievements greatly promote the possibilities that can directly generate the self-sweeping effect in other doped fibers. Lobach *et al.* uncovered the bismuth, thulium, neodymium self-sweeping fiber lasers[12–14]. Peterka *et al.* revealed the erbium and holmium self-sweeping fiber lasers[15,16]. Wang *et al.* contributed to the thulium–holmium co-doped self-sweeping fiber laser[17]. These new wavebands greatly expand the applications of spectral detection and analysis[13,18,19]. Especially, the self-sweeping thulium fiber laser provides a better platform for studies of the self-sweeping effect due to the wider sweeping range and numerous applications near 1.9 μm. Among the self-sweeping fiber lasers, the single-frequency output strictly obeys the behaviors of the simulated curve and exhibits excellent performance in pulse shape and spectral shift, which has been applied in the generation of short pulses based on Fourier synthesis[20].

However, this effect still gets studied for fresh phenomena. In 2016, Navratil *et al.* first, to the best of our knowledge, reported Yb-doped self-sweeping with multiple sweeping regimes. As the pump power increases, the fiber laser undergoes reverse, hybrid, and normal self-sweeping operations[21]. The wavelength shifting direction is a criterion for distinguishing the self-sweeping regime, i.e., the increase and decrease in wavelength represent the normal and reverse regimes, respectively. Two years later, Budarnykh *et al.* reported the evolution of sweeping regimes in the thulium fiber laser, while reverse, stopping, and normal sweeping were engendered in sequence[22]. Further high-resolution analysis unveiled that the reverse sweeping and wavelength stopping signify the reverse shift and stop of the sweeping range, respectively. The significant observation is that only normal sweeping occurred in such a sweeping range[23]. To date, the mysterious spectral dynamics of self-sweeping have been revealed and analyzed by the gain–loss profile. The self-sweeping fiber laser has brought about numerous advances and is still developing new branches. In 2019, the bidirectional operated self-sweeping thulium fiber laser was introduced splendidly by Jiang *et al.*[24]. The salient feature is that the sweeping rate slowed down in a reverse self-sweeping regime with the ascending pump power. Our previous works also made a contribution to this feature of the ytterbium fiber laser[25,26]. The bidirectional structure also provides a platform for the study of the reverse self-sweeping effect.

Throughout development of the self-sweeping effect, the outstanding spectral shift is our pursuant goal. Actually, researchers obtained a rather narrow sweeping range in various doped fiber lasers except for the Yb and thulium fiber lasers. To generate and control the sweeping range, the length and temperature of active fiber, the temperature of the laser diode (LD), output mirror losses, the ratio of couplers, and the temperature of the Lyot filter can be adjusted in the laser cavity for optimizing self-sweeping performance[9,10,26]. However, the complex operation and high cost still restrict further exploration. In this Letter, we report a wavelength-flexible all-polarization-maintaining (PM) self-sweeping fiber laser based on the intracavity loss tuning brought by the bent fiber circle. The self-sweeping effect is achieved by the bidirectional operated laser cavity. The diameter of the circle provides the tuning of losses. The sweeping range can cover 1055.6–1034.6 nm with the decrease of diameter, and the initial wavelength decreases and threshold power increases at the same time. The easy approach has the potential to promote the improvement of sweeping performance in various doped fiber lasers without additional consumption and cost.

2. Experimental Setup and Measurement

2.1. Measurement of bent fiber circle

The setup for measuring amplified stimulated emission (ASE) spectra is shown in Fig. 1(a). The PM LD connects with the reflecting port of PM wavelength division multiplexer (WDM) and provides 150 mW pump power. One port of a 1.3 m PM Yb fiber connects with the common port of the PM WDM. The other port connects with a section of PM fiber with a bent fiber circle (PM980 PANDA). The spectral characteristics were investigated by the use of an optical spectrum analyzer (OSA, Yokogawa, AQ6370C). In this measurement, the diameter of the fiber circle is controlled via wrapping the fiber around various cylinders with different diameters in only one circle. Figure 1(b) shows the ASE output spectra via different cylinders. One can see that the diameter of the circle is controlled to reduce the bandwidth and intensity of the ASE spectra. The curvature loss of the PM fiber is exhibited in Fig. 2. The measured data obey the fitting curve that was fitted by the derived formula in Ref. [27]. The lower diameter possesses larger losses. When the diameter was set as 4 mm (black line), the ASE spectrum disappeared. With the diameter beyond 18 mm, the ASE spectra are constant, as shown in the inset. As a comparison, for the ASE of the erbium fiber, the descending bent diameters lead to the peak of gain shift to a shorter wavelength under a constant pump power. Therefore, the tunable- or dual-wavelength fiber laser can be achieved by the use of the attenuator, the fiber coils, and bent fiber[28–33]. However, although the obvious shift does not occur as the pump power changes in the Yb fiber, the increasing of intracavity losses leads to requirement of a pump power increase, which leads, in turn, to maximum gain

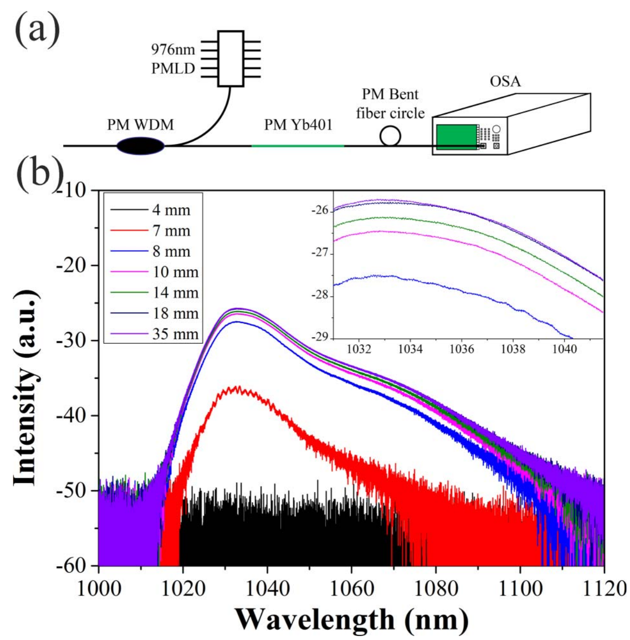

Fig. 1. (a) ASE measurement setup. (b) The ASE spectra in different diameters of bent fiber circles.

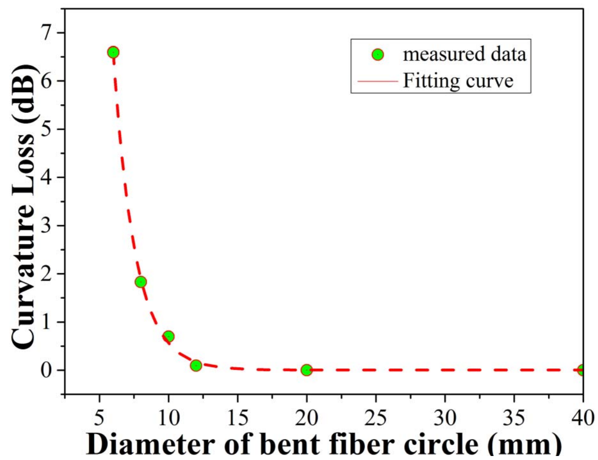

Fig. 2. Relationship between the curvature loss and the diameter of the bent fiber circle.

wavelength reduction. The first attempt of intracavity loss tuning in the self-sweeping fiber laser was performed in Ref. [9], where the reflection of the output mirror provided variable loss. However, this way is not suitable for the bidirectional cavity. Thereby, we propose the bent fiber to act as the device for intracavity loss tuning to expand the reverse sweeping range in the bidirectional cavity.

2.2. Experimental setup

Figure 3 shows the experimental setup of the proposed fiber laser. The PM LD serves as a pump source to generate the radiation of 976 nm that passes through the reflecting and common ports of the PM WDM and can be absorbed by the 1.3 m long PM Yb fiber. The clockwise (CW) ASE output experiences the output coupler, bent fiber circle, and PM WDM. The counter-CW(CCW) ASE output takes the opposite path. Both the PM WDM and PM coupler have broad operating range (1020–1090 nm), which assures the tunability of the fiber laser. The active fiber provides core absorption of 140 dB/m at 915 nm and numerical aperture of 0.14. The diameters of the mode field, cladding, and coating are 6, 125, and 250 μm, respectively.

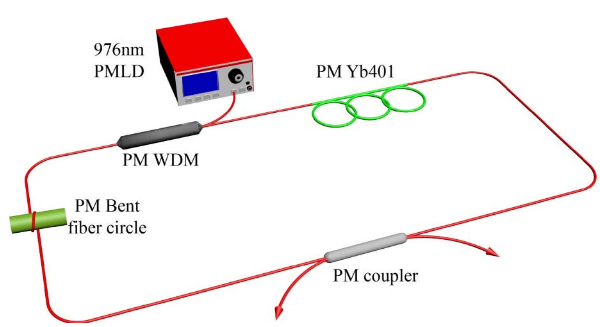

Fig. 3. Experimental setup of the proposed all-PM fiber laser. PM LD, polarization-maintaining laser diode. PM WDM, polarization-maintaining wavelength division multiplexer. PM Yb401, polarization-maintaining ytterbium-doped fiber.

A 2 × 2 3 dB coupler is used as the output coupler, which connects the APC jumper for the measurement. The length of the whole cavity is about 4.5 m.

3. Expermiental Results and Discussion

The temporal dynamics of the proposed fiber laser can be monitored by two detectors (Thorlabs DET08CFC) and an oscilloscope (Agilent Technology DPO9104A). Figure 4 exhibits the typical intensity dynamics of our fiber laser without extra loss under a 50 mW pump power. Figure 4(a) shows the microsecond pulse of ~40 kHz repetition frequency. The iconic feature of bidirectional self-sweeping fiber laser shown in Fig. 4(b) depicts the phase difference between the CW signal and CCW signal, which can be attributed to the reflection and transmission of the induced dynamic grating along the active fiber[26]. The longitudinal beating signal can be distinguished as 22 ns, in which the interval of the longitudinal mode is about ~45.5 MHz. Therefore, the length of our cavity can be calculated as 4.48 m, which is coincident with our measured length. Interestingly, the pulse average repetition frequency is nearly constant when the pump power was set, which is immune to the tuning losses except for the obvious change in intensity.

Figure 5 shows the threshold power and the initial wavelength characteristics of the wavelength-flexible self-sweeping fiber

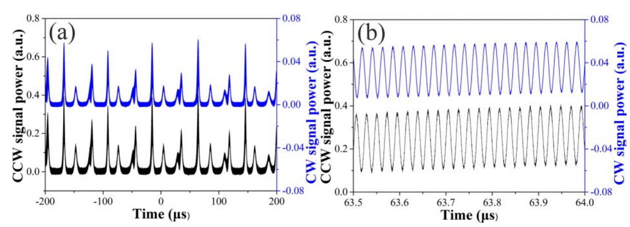

Fig. 4. Intensity dynamics of bidirectional all-PM self-sweeping Yb-doped fiber: (a) the microsecond pulse, (b) the zoomed view.

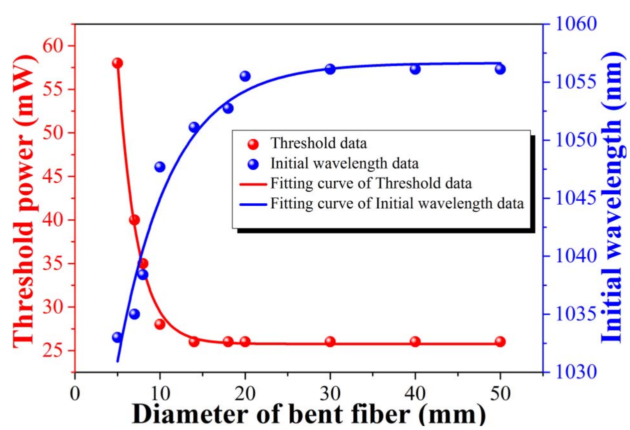

Fig. 5. Relationship between the diameter of the bent fiber circle and both threshold power and initial wavelength.

laser, with the diameter of the bent fiber circle ranging from 4 mm to 50 mm. One can see that the different sweeping regimes with different threshold powers and initial wavelengths possess the different sweeping range. Visibly, the characteristics are related to the loss brought by the bent fiber circle. Therefore, the equation below can be used to express the relation between the diameter of the bent fiber circle and both threshold power and initial wavelength clearly:

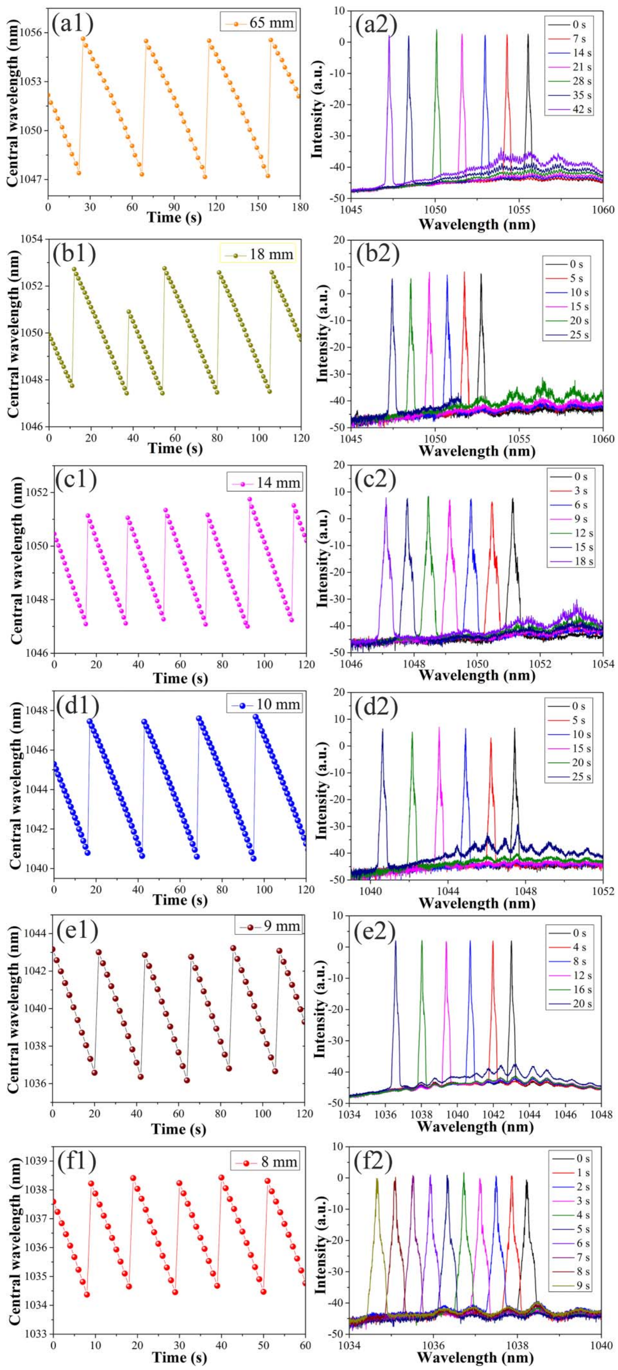

Fig. 6. Iconic spectral dynamics of self-sweeping regimes in different diameters of bent fiber circles: (a1) and (a2) 65 mm; (b1) and (b2) 18 mm; (c1) and (c2) 14 mm; (d1) and (d2) 10 mm; (e1) and (e2) 9 mm; (f1) and (f2) 8 mm.

$$y = \frac{\pm a}{\sqrt{r}} e^{-\frac{r}{b}} + y_0, \tag{1}$$

where a and b are constants related to the bent fiber parameters (a is positive in threshold fitting and negative in initial wavelength fitting)[31]. y represents the pump power or the initial wavelength. y_0 expresses the value of pump power or the initial wavelength without bent loss. r is the diameter of the bent fiber circle. The experimental result is fitted by the equation perfectly, which also manifests that the intracavity loss tuning can cover a broad wavelength range. However, one can see that the initial wavelength is located at 1055.6 nm without bending loss, which is determined by the parameters of our cavity, including the length of the cavity, the ratio of output coupler, and so on. Although we can replace the parameters to make self-sweeping occur at a longer wavelength while we prepared the experiment, we still selected the experimental parameters used in the paper to avoid the emergence of ultra-slow self-sweeping[26].

Figure 6 displays the iconic spectral dynamics of a reverse self-sweeping fiber laser with different bent fiber circles. The sweeping range tends to the shorter wavelength when the diameter of the bent fiber circle decreases, along with the ascending sweeping rate. When the diameter goes down under 4 mm, the initial wavelength decreases steadily, but the self-sweeping effects are not obvious. The increasing threshold of the fiber laser cuts down the length of the unpumped active fiber that lessens the absorption of shorter wavelengths (due to the long active fiber and low pump power), which therefore further reduces the maximal gain wavelength. This leads to the sweeping range finally moving toward the shorter wavelength.

The intuitive description of the results of Fig. 6 is depicted in Fig. 7. Figure 7(a) presents the start and stop wavelengths with sweeping periods, in which the two sets of data can be well fitted by Eq. (1), and the corresponding sweeping rate and selected pump power are marked in Fig. 7(b). The selected pump powers for measuring the data of self-sweeping are beyond the 1.5 times threshold in order to obtain the broader sweeping range. The behavior of the sweeping range in our experiment also accords with the trend that is generated by the intracavity loss variation involved with Ref. [9]. One interesting behavior that can be found is that the sweeping rate increases when the sweeping range moves to the shorter wavelength, which is an analogue with our previous work[26]. However, the reason is still not clear. Further studies are still required for this effect.

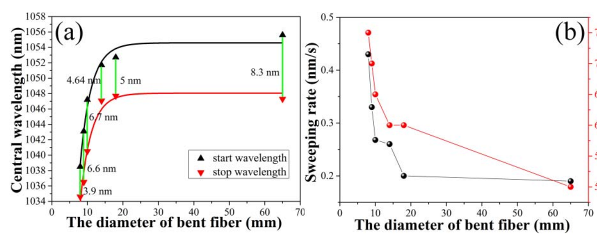

Fig. 7. (a) Relationship of start and stop wavelengths and (b) sweeping rate and selected pump power varying with the bent diameter.

4. Conclusion

In summary, we reported a wavelength-flexible all-PM self-sweeping fiber laser via the bent fiber circle. The tuning sweeping range can be achieved by controlling the diameter of THE bent fiber circle effectively. In this experiment, the self-sweeping output ranged from 1055.6 nm to 1034.6 nm with high optical signal-to-noise ratio (OSNR). Both the threshold power and initial wavelength followed the criterion of Eq. (1). Our study provides a simple and effective way to obtain a wide self-sweeping operation in various doped fiber lasers and has the potential to promote the application of spectral measurement and analysis.

Acknowledgement

This work was supported by the National Natural Science Foundation of China (No. 61905193), the National Key R&D Program of China (No. 2017YFB0405102), and the Key R&D Project of Shaanxi Province–International Science and Technology Cooperation Project (No. 2020KW-018).

References

1. T. P. Hughes and K. M. Young, "Mode sequences in ruby laser emission," Nature **196**, 332 (1962).
2. V. Kir'yanov and N. Il'ichev, "Self-induced laser line sweeping in an ytterbium fiber laser with non-resonant Fabry–Perot cavity," Laser Phys. Lett. **8**, 305 (2011).
3. P. Peterka, P. Navrátil, J. Maria, B. Dussardier, R. Slavík, P. Honzátko, and V. Kubeček, "Self-induced laser line sweeping in double-clad Yb-doped fiber-ring lasers," Laser Phys. Lett. **9**, 445 (2012).
4. I. A. Lobach, S. I. Kablukov, E. V. Podivilov, and S. A. Babin, "Self-scanned single-frequency operation of a fiber laser driven by a self-induced phase grating," Laser Phys. Lett. **11**, 045103 (2014).
5. I. A. Lobach, S. I. Kablukov, E. V. Podivilov, and S. A. Babin, "Broad-range self-sweeping of a narrow-line self-pulsing Yb-doped fiber laser," Opt. Express **19**, 17632 (2011).
6. P. Peterka, P. Honzátko, P. Koška, F. Todorov, J. Aubrecht, O. Podrazký, and I. Kašík, "Reflectivity of transient Bragg reflection gratings in fiber laser with laser-wavelength self-sweeping," Opt. Express **22**, 30024 (2014).
7. P. Peterka, P. Koska, and J. Ctyroky, "Reflectivity of superimposed Bragg gratings induced by longitudinal mode instabilities in fiber lasers," IEEE J. Sel. Top. Quantum Electron. **24**, 902608 (2018).
8. R. R. Drobyshev, I. A. Lobach, E. V. Podivilov, and S. I. Kablukov, "Spectral characterization technique of self-organized distributed feedback in a self-sweeping fiber laser," Opt. Express **27**, 21335 (2019).
9. I. A. Lobach, A. Y. Tkachenko, and S. I. Kablukov, "Optimization and control of the sweeping range in an Yb-doped self-sweeping fiber laser," Laser Phys. Lett. **13**, 045104 (2016).
10. R. V. Drobyshev, I. A. Lobach, and S. I. Kablukov, "Narrow-linewidth self-sweeping fiber laser with scanning range control by a tunable Lyot filter," Laser Phys. **29**, 105104 (2019).
11. A. Y. Tkachenko, A. D. Vladimirskaya, I. A. Lobach, and S. I. Kablukov, "Michelson mode selector for spectral range stabilization in a self-sweeping fiber laser," Opt. Lett. **43**, 1558 (2018).
12. I. A. Lobach, S. I. Kablukov, M. A. Melkumov, V. F. Khopin, S. A. Babin, and E. M. Dianov, "Single-frequency bismuth-doped fiber laser with quasi-continuous self-sweeping," Opt. Express **23**, 24833 (2015).
13. A. E. Budarnykh, A. D. Vladimirskaya, I. A. Lobach, and S. I. Kablukov, "Broad-range self-sweeping single-frequency linearly polarized Tm-doped fiber laser," Opt. Lett. **43**, 5307 (2018).
14. E. K. Kashirina, I. A. Lobach, and S. I. Kablukov, "Single-frequency self-sweeping Nd-doped fiber laser," Opt. Lett. **44**, 2252 (2019).
15. P. Navratil, P. Peterka, P. Vojtisek, I. Kasik, J. Aubrecht, P. Honzatko, and V. Kubecek, "Self-swept erbium fiber laser around 1.56 μm," Opto-Electron. Rev. **26**, 29 (2018).
16. J. Aubrecht, P. Peterka, P. Koška, O. Podrazký, F. Todorov, P. Honzátko, and I. Kašík, "Self-swept holmium fiber laser near 2100 nm," Opt. Express **25**, 4120 (2017).
17. X. Wang, P. Zhou, X. Wang, H. Xiao, and L. Si, "Tm–Ho co-doped all-fiber brand-range self-sweeping laser around 1.9 μm," Opt. Express **21**, 16290 (2013).
18. A. Y. Tkachenko, I. A. Lobach, and S. I. Kablukov, "All-fiber Brillouin optical spectrum analyzer based on self-sweeping fiber laser,"; Opt. Express **25**, 17600 (2017).
19. I. A. Lobach and S. I. Kablukov, "Application of a self-sweeping Yb-doped fiber laser for high-resolution characterization of phase-shifted FBGs," J. Lightwave Technol. **31**, 2982 (2013).
20. I. A. Lobach, S. I. Kablukov, E. V. Podivilov, A. A. Fotiadi, and S. A. Babin, "Fourier synthesis with single-mode pulses from a multimode laser," Opt. Lett. **40**, 3671 (2015).
21. P. Navratil, P. Peterka, P. Honzatko, and V. Kubecek, "Reverse spontaneous laser line sweeping in ytterbium fiber laser," Laser Phys. Lett. **14**, 035102 (2017).
22. A. E. Budarnykh, I. A. Lobach, and S. I. Kablukov, "Self-sweeping Tm-doped fiber laser with wavelength stopping," Laser Phys. Lett. **16**, 025108 (2019).
23. A. E. Budarnykh, A. D. Vladimirskaya, I. A. Lobach, and S. I. Kablukov, "High-resolution analysis of wavelength stopping effect in a self-sweeping fiber laser," Laser Phys. Lett. **16**, 085104 (2019).
24. H. B. Jiang, Z. H. Zhao, L. Jin, S. Y. Set, and S. Yamashita, "Self-wavelength-sweeping in a bi-directional thulium-doped fiber ring laser," Appl. Phys. Express **12**, 042006 (2019).
25. K. L. Wang, Z. R. Wen, X. Y. Qi, B. L. Lu, and J. T. Bai, "Wavelength self-sweeping Yb-doped bi-directional fiber ring laser," Proc. SPIE **11209**, 112092I (2019).
26. K. L. Wang, Z. R. Wen, H. W. Chen, X. Y. Qi, B. L. Lu, and J. T. Bai, "Observation of reverse self-sweeping effect in an all-polarization-maintaining bidirectional ytterbium-doped fiber laser," Opt. Express **28**, 13913 (2020).
27. D. Marcuse, "Curvature loss formula for optical fibers," J. Opt. Soc. Am. **66**, 216 (1976).
28. X. Zhao, Z. Zheng, L. Liu, Y. Liu, Y. Jiang, and X. Yang, "Switchable, dual-wavelength passively mode-locked ultrafast fiber laser based on a single-wall carbon nanotube modelocker and intracavity loss tuning," Opt. Express **19**, 1169 (2011).
29. H. B. Jiang, Y. P. Huang, Z. H. Zhao, T. Shirakata, L. Jin, S. Y. Set, and S. Yamashita, "Laser mode locking using a single-mode-fiber coil with enhanced polarization-dependent loss," Opt. Lett. **45**, 2866 (2020).
30. S. X. Chen, Y. H. Chen, K. Liu, R. Sidharthan, H. Z. Li, C. J. Chuang, Q. J. Wang, D. Y. Tang, and S. W. Yoo, "All-fiber short-wavelength tunable mode-locked fiber laser using normal dispersion thulium-doped fiber," Opt. Express **28**, 17570 (2020).
31. Y. Zhu, F. Xiang, L. Jin, S. Y. Set, and S. Yamashita, "All-fiber dual-wavelength mode-locked laser using a bend-induced-birefringence Lyot-filter as gain-tilt equalizer," IEEE Photon. J. **11**, 1504807 (2019).
32. H. Chen, X. Jiang, S. Xu, and H. Zhang, "Recent progress in multi-wavelength fiber lasers: principles, status, and challenges," Chin. Opt. Lett. **18**, 041405 (2020).
33. K. Y. Lau, P. J. Ker, A. F. Abas, M. T. Alresheedi, and M. A. Mahdi, "Mode-locked fiber laser in the C-band region for dual-wavelength ultrashort pulses emission using a carbon nanotube saturable absorber," Chin. Opt. Lett. **17**, 051401 (2019).